Digitally Controlled Switch-Mode Power Driver for Active Magnetic Bearings

Tomer Ben-Moha, Sergei Basovich, Mor Mordechai Peretz, Shai Arogeti, and Ziv Brand
Ben-Gurion University of the Negev, P.O.B 653 Beer-Sheva 84105, Israel
Email: benmohat@post.bgu.ac.il

***Abstract*—This paper presents the concept and the practical implementation of a switch-mode power driver for the use in Active Magnetic Bearings (AMB). The switch-mode driver consists of a full-bridge capable of operating in 2-level, 3-level, or phase-shifted PWM mode. An optimal digital current-programmed mode controller lays out the foundations to a proximate-optimal, robust, large-signal dynamic response of the system under extreme cases of loading and parameters variations. In particular, the developed power driver is capable of following the desired reference for large inductance variations (due to displacement). The power stage combines a newly developed, efficient, passive-based current sensor that is capable of sensing bi-directional and near-zero currents, while being robust to external disturbances and maintaining simple and efficient structure. Performance evaluation of the power driver has been verified experimentally on a closed-loop design for a single-axis AMB platform using a dual channel prototype, controlled using a single 16-bit, low-cost microcontroller.**

I. Introduction

The key factor that is required for reliable operation for Active Magnetic Bearings (AMB) is a well-regulated current-sourcing power driver with low quiescent noise to assure steady-state stability [1]. Another requirement is that the power driver is capable to sustain large-signal load variations, and follow a desired reference with guaranteed dynamic performance under wide changes in the system parameters. The latter is due to the fact that the effective inductance of the actuator significantly varies with the displacement of the rotor [2],[3].

Two general types of power drivers exist in the literature in the context of AMB. One approach is based on the classic linear amplifiers, and it is inherently associated with very poor efficiency [4]. The more preferred approach to drive magnetic actuators is by switch-mode converters technology which has a proven superiority in terms of efficiency and reduced size at the cost of a larger, yet still acceptable, quiescent noise [5]. To further reduce the steady-state noise, a three-level PWM mode of operation is commonly used [2],[6],[7],[8],[9],[10],[11]. However, the controller implementation may become complex, in particular when multiple actuators per control-axis are required.

Following the recent growth in popularity of digital control, adaptation of control concepts from motor drives and switch-mode power supplies (SMPS) applications that were applied to AMB systems, have demonstrated conceptual operation with good dynamic performance [12]. However, as in the initial steps in digital control of SMPS [13],[14] similar to analog control, operation is obtained using high-performance microprocessors which makes this type of solution economically-prohibitive, in particular for lower power AMB systems.

Another important element in the design of current-sourcing converter for AMB is the current sensor. Although the subject of current sensing has not been widely addressed hitherto, it is a key factor to assure the desired performance, especially for the case of switching systems. In [15], the actuator current is sensed via a series resistor, therefore introducing additional losses. These can be eliminated using a hall-effect device [8], [16], at the cost of sensitivity to external magnetic fields and more complex design. However, both methods exhibit poor SNR at lower current levels. Since the nonlinear AMB plants are usually controlled using the feedback linearization method [17], which involves the on-off switching of the opposite electromagnets, the capability of the proper near-zero currents sensing is crucial to the reliable AMB system operation. An alternative approach to current sensing derived from SMPS technology that is pursued in this study is using a current transformer. Here, the current of the switching element is passed via a pulse transformer and the full behavior of the signal is restored using additional circuitry. The main limitation of such design is associated with a reset of the pulse transformer [18].

The objective of this study is thus to introduce an efficient current-sourcing driver for AMB applications with fully-integrated digital current-programmed mode controller and a newly developed digital-control-oriented current sensing method using a simple pulse transformer. The power driver system described in Fig.1 for two-channel design consists of two H-bridge converters, synchronously operating in a three-level PWM mode, governed and controlled by a single 16 bit, fixed-point, microcontroller. The driver exhibits robust response for changes in the reference, loading conditions and system parameters.

The paper is organized as follows; the power module structure and principle of operation, as well as the description of the new current sensing method are given in Section II. The discrete optimal controller design is described in Section III. Section IV presents the experimental results, and Section V concludes the paper.

978-1-4799-5776-7/14/$31.00

II. Power Driver Overview

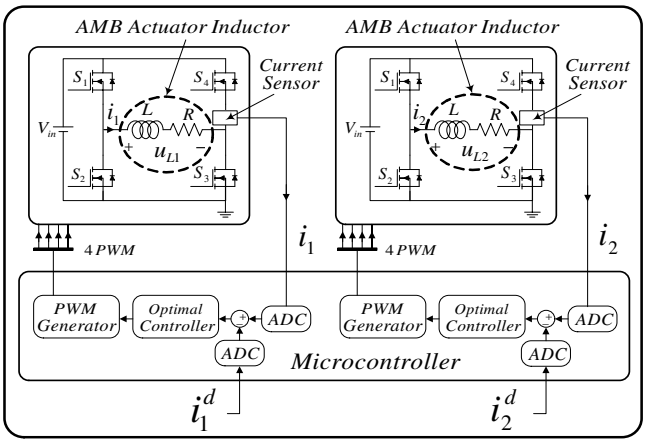

Fig. 1: Schematic description of two-channel power driver

A. Structure and Operating Principle

The switch-mode power driver (Fig.1) consists of eight MOSFETs, each four of them in H-bridge configuration, and a microcontroller capable of sampling voltage using A/D and generating 8 PWM signals.

According to schematic representation in Fig.1 the microcontroller ADC samples the inductor current and reference current signals at a predefined rate, which in this study is chosen to be at the switching frequency (upper bound of the switching system) to allow rapid response of the controller. The calculated error between the measured currents i_1, i_2 and the desired currents i_1^d, i_2^d is then serves as an input to the optimal current-control algorithm developed to produce the required correction signal such to regulate the average actuator current PWM signals (S_1, S_2, S_3, S_4 where S_2,S_4 are complimentary to S_1,S_3 respectively) at the switching frequency of 100[kHz] for two H-bridges, which are produced simultaneously using a dedicated per-converter PWM generator. The notation L, R, V_{in} is used to represent the actuator inductance, parasitic resistance and input voltage, respectively. The voltage between the actuator terminals in both H-bridges is denoted by u_{L1} and u_{L2}. As it can be observed from Fig.1, the current regulation depends on the capability of accurately sensing actuator's current. To this end, a simple and efficient current sensor based on a pulse transformer, has been developed and is detailed in the following section.

B. Current Sensing Method

Accurate current measurement is essential to assure the desired closed-loop performance of the power driver. Similarly to inductor current sensing in SMPS, the main challenge in sensing the actuator's current, is the need to measure the DC component, which cannot be applied using simple current transformers. To this end, numerous current sensing methods for switch-mode applications have been covered in the literature, among them sense resistor [19], Hall-effect [20] and current transformers paired with signal reconstruction circuits [18]. However, in the context of AMB applications, the realization of current sensors has been conventionally applied by either resistive or Hall-effect concepts due to their capability to obtain both the AC and DC components of the signal. The main drawbacks of resistive measurement are the introduction of additional losses in the conduction path, poor signal-to-noise ratio at lower currents, and that they require instrumentation with relatively high common-mode rejection ratio. Simple Hall-effect devices are prone drifts and are sensitive to external magnetic fields and nearby currents [20].

Current transformers are limited to AC measurements due to the need for flux balance (i.e. reset) to avoid saturation of the magnetic element. DC measurement via a transformer conventionally applies a reset circuitry, similar to the operation of a forward converter [18], i.e. the DC current is passed through the transformer in intervals sufficiently spaced to allow balancing of the flux. One possible implementation, widely used in SMPS applications (Fig.2) is to locate the primary winding of current transformer in series to a switching element and a diode in series to the measurement (on a resistor) at the secondary winding. In this way, the peak value of the pulsating current is accurately obtained during the conduction time of the switch and the reset of the transformer is facilitated during its off interval, however, the voltage developed at the secondary winding during the reset interval may be significantly high. By reversing the reset concept, another possible solution is the transformer-based current sense circuit that has been presented in [19] and further advanced in [21] for compatibility with digital control operation. There, DC current of the primary winding is obtained using an AC equivalent of the secondary winding. An external excitation in the secondary winding alternates the current, creating a pulsed waveform with peak current that is proportional to primary DC value. Assuming negligibly small ripple, a snapshot of the signal per sampling interval is sufficient data to reconstruct the actual current waveform. In addition to isolation, this method offers the possibility to directly measure the DC current through the actuator, however, it requires additional timing and control circuitry. Another drawback of both solutions in the context of AMB is the incapability to sense both positive and negative currents, which reflects on the ability to set the actuatorâĂŹs current on zero. This property is essential in order to implement the commonly used feedback linearization control law in AMB [17].

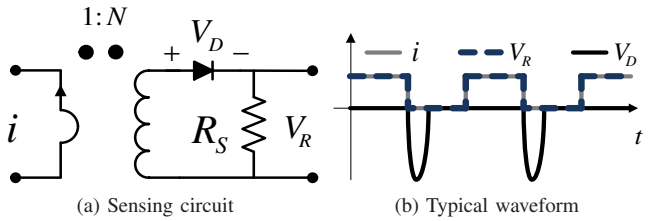

(a) Sensing circuit (b) Typical waveform

Fig. 2: DC current transformer sensing

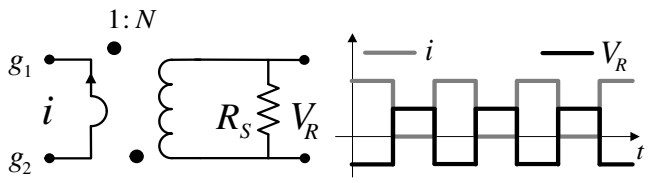

(a) Sensing circuit (b) Typical waveform

Fig. 3: Introduced transformer sensing

In this study, a modified approach, that combines the benefits of the above-mentioned current transformer based methods with the benefits of a digital control, has been developed. The description of the sensor and its principle of operation is assisted by Fig.3, Fig.4 and Fig.5.

As shown in Fig.3a, a conventional AC current transformer is realized to obtain the pulsating current shape of the switch current. The primary winding is connected in series to the switch and the current value is obtained on a resistor at the secondary winding. Since the original signal has a DC component, which is not passed through the transformer (Fig.3b), the relationship between the primary and the secondary peak currents depends on the duty ratio $(1 - D)$ of the switch, and is expressed as:

$$i_{sec} = \frac{i_{avg} - i}{N} = \frac{-D\,i}{N}, \tag{1}$$

where i_{avg} is the DC component, N is the winding ratio of the transformer and D is the duty cycle of S_1 and S_3.

The operation of an AMB involves both positive and negative current through the actuator, depending on the duty ratio of the H-bridge. To allow acquisition of both negative and positive current values using an ADC, a fixed DC value, V_0, is added to the signal as can be observed in Fig.4. The sensed signal by the ADC, V_{ADC} can be expressed as:

$$V_{ADC} = \left(\frac{R_1 + R_2}{R_1}\right) V_0 + \left(\frac{R_2}{R_1}\right) \frac{R_S}{N}\, D\, i \tag{2}$$

where R_S is the resistor on which the secondary current convert to voltage, R_1 and R_2 are the resistors that sets the gain of the amplifier.

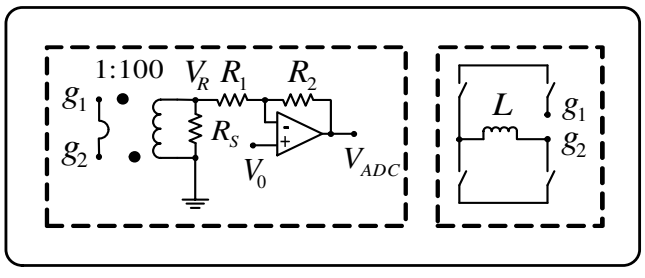

Fig. 4: The introduced current sensor and its location in the H-bridge circuit

Since the entire controller operation is facilitated digitally, the current duty ratio of all switches is available at all times. For a given D, the real DC value of the actuators current can be determined by:

$$i_{ADC} = \left[V_{ADC} - \left(\frac{R_1 + R_2}{R_1}\right) V_0\right] \frac{R_1}{R_2} \frac{N}{R_S} \frac{1}{D} \tag{3}$$

which can be obtained using the ADC within the entire conduction time frame of the switch.

Fig.5 illustrates a detailed timing diagram and key waveforms of the introduced current sensor for various operating points of the power driver. Due to V_0 offset, the actuator current can be successfully restored for both negative ($V_R > 0$) and positive ($V_R < 0$) current values. Using the current sensing method described here, the following advantages are obtained: no additional losses in the conduction path, galvanic isolation, simple realization without special instrumentation, EMI immunity, and lowered reset voltage compared to other solutions.

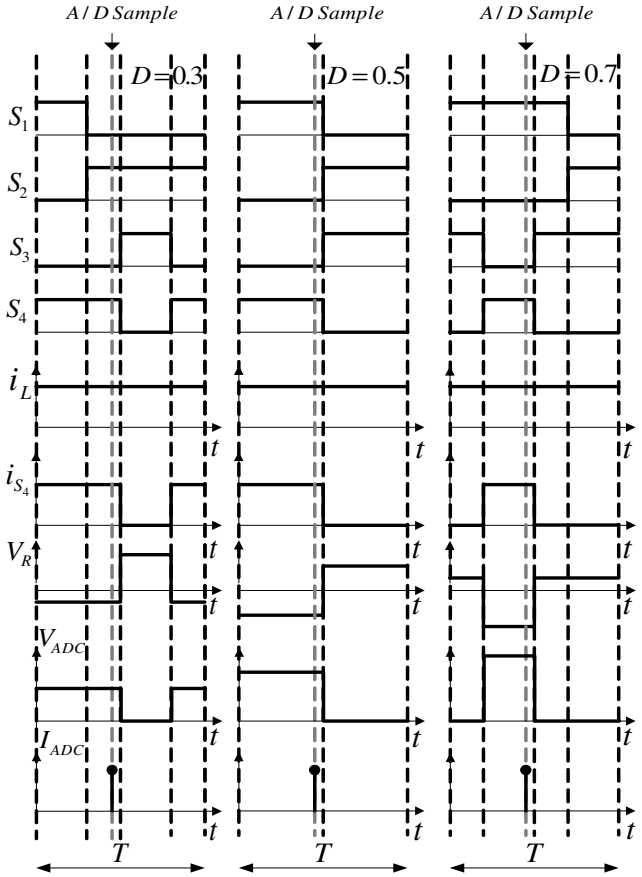

Fig. 5: Current sampling principle for a variety of PWM signals (T is the sampling period, S_2 and S_4 are complimentary to S_1 and S_3 respectively)

III. Controller Design

This section is devoted to the optimal discrete controller design. In view of [22], the controller is designed for the regulation case. Following [9], the relation between the coil voltage and current can be described by

$$\frac{di}{dt} + \frac{R}{L} i = \frac{u_L}{L} \tag{4}$$

Define the control signal u as follows

$$u = 2D - 1, \quad -1 < u < 1 \tag{5}$$

where D is the duty cycle of S_1 and S_3. Assuming that the MOSFETs inner resistance is negligible, using (5) we rewrite (4) as

$$\frac{di}{dt} + \frac{R}{L} i = \frac{V_{in}}{L} u \tag{6}$$

The following state variables

$$x_1 = \int_0^t i(\tau) d\tau, \quad x_2 = i \tag{7}$$

are used to obtain the state space representation of (6)

$$\dot{x} = Ax + Bu, \quad y = Cx \tag{8}$$

where $x \triangleq \{x_1, x_2\}^T$, and

$$A \triangleq \begin{bmatrix} 0 & 1 \\ 0 & -\frac{R}{L} \end{bmatrix}, \; B \triangleq \begin{bmatrix} 0 \\ -\frac{V_{in}}{L} \end{bmatrix}, \; C \triangleq \begin{bmatrix} 0 & 1 \end{bmatrix} \tag{9}$$

Assuming that the sampling period T is small with respect to the system bandwidth, the first order approximation can be used to represent the system (8)-(9) in discrete state space by

$$x(k+1) = A_d x(k) + B_d u(k), \quad y(k) = Cx(k) \tag{10}$$

$$A_d \triangleq I + AT, \quad B_d \triangleq BT \tag{11}$$

where I is identity matrix. Application of discrete linear quadratic regulation (LQR) methodology yields the control law of the form

$$u(k) = -Kx, \quad K = (B_d^T S B_d + R)^{-1} B^T S A_d \quad S, R > 0 \tag{12}$$

which minimizes the following cost function

$$J(u) = \sum_{n=1}^{\infty} (x(k)^T Q x(k) + u(k)^T R u(k)) \tag{13}$$

where $S > 0$ solves the algebraic Riccati equation

$$A_d^T S A_d + Q - S - A_d^T S B_d (B_d^T S B_d + R)^{-1} B^T S A_d = 0 \tag{14}$$

It can be verified that for $T = 1 \times 10^{-5}$ [sec] and for L, R, V_{in} that are given in Section II, the following holds

$$rank \{B_d, \; A_d B_d\} = 2 \tag{15}$$

therefore a couple $\{A_d, B_d\}$ is controllable. Since a couple $\{A_d, C\}$ is not observable, in order to assure stability of (10)-(11) with (12) the weight matrix Q must be chosen in such a way that a couple $\{A_d, Q\}$ will be detectable [23]. In other words Q have to satisfy [24]

$$\exists P > 0 \quad | \quad A_d^T P A_d - P - Q^T Q < 0 \tag{16}$$

Thus, solving (14) for

$$Q = \begin{bmatrix} 2.3575e8 & 0 \\ 0 & 37 \end{bmatrix}, \quad R = 0.1 \tag{17}$$

one can obtain the following control gain

$$K = \begin{bmatrix} 3599.2 & 18 \end{bmatrix} \tag{18}$$

IV. Experimental Results

This section presents performance evaluation experiments which conducted on both an isolated power driver and a 1-DOF AMB system driven by the power driver.

A. Desired Current Tracking

The operation of the power driver has been experimentally validated using a 2-channel prototype (Fig.6) as described in Fig.1, operating at 100 [kHz].

The system parameters were: $L = 17 - 45$ [mH], $R = 1.6$ [Ω], $V_{in} = 25$ [V]. The digital controller has been implemented with a single 16-bit, fixed-point, microcontroller that comprises a 10-bit ADC, and eight PWM outputs.

The power driver performance was validated for both set-point and sinusoidal wave tracking. The results of the experiments are shown in Fig.8a and Fig.8b. An experimental demonstration of the current sensing method is shown in Fig.7.

In order to evaluate the dynamic performance of the power driver the relevant performance measure of the power amplifier should be obtained observing the response to a large-signal perturbation. Thus, the information available from the small-signal bode plot can lead to deceptive conclusions. On the other hand, the large-signal dynamic characteristics of the power amplifier can be estimated using the rise time of the response in Fig.8a as follows: $\omega_{BW} = 2/t_r$, where ω_{BW} [rad/sec] is the equivalent bandwidth, and $t_r = 1.5$ [msec] is the rise time.

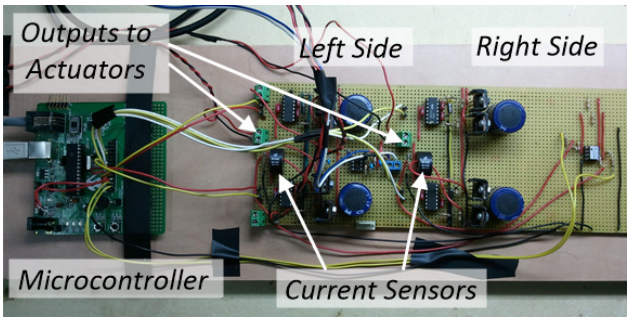

Fig. 6: Power driver

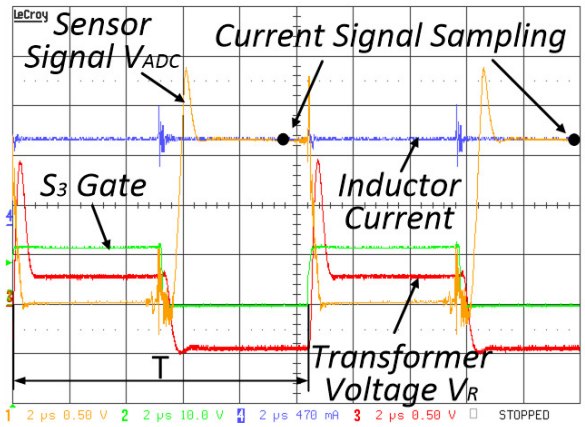

Fig. 7: Current sampling point with respect to other signals

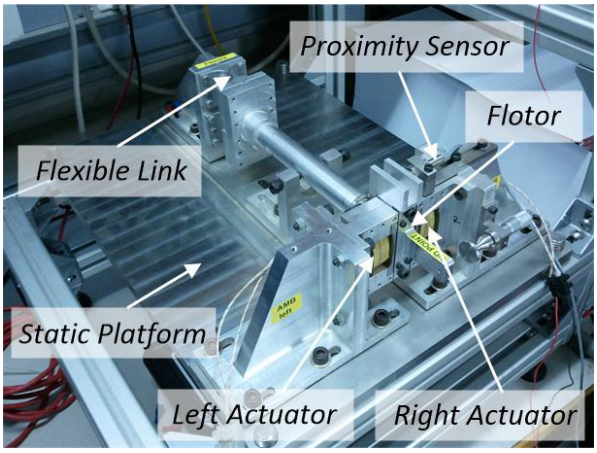

Fig. 9: Single-axis AMB system

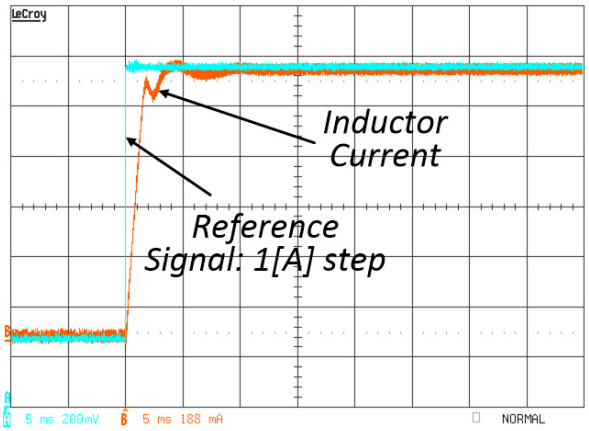

(a) Step response

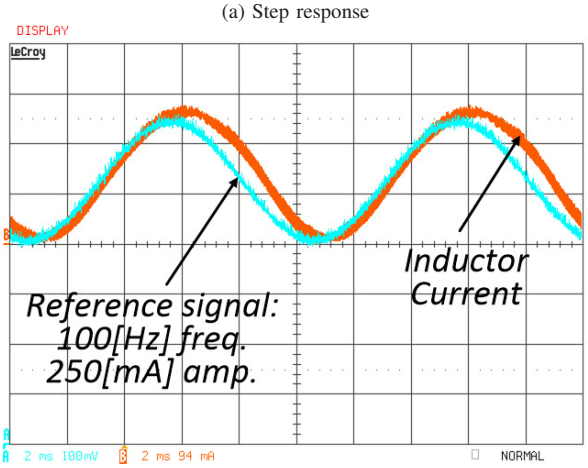

(b) Sinusoidal signal traking

Fig. 8: Desired current tracking

B. AMB System Driving

A single-axis AMB system (Fig.9) was used to test the presented power driver performance. This AMB system consists of two electromagnets, a moving part, a static part and a proximity sensor. The moving part is connected to the static platform by a flexible link, the displacement of the moving part is measured by the proximity sensor. The parameters of the AMB testbed are shown in Tab.I. The AMB control loop was implemented using the MATLAB real-time toolbox and an acquisition card. The performed experiments include tracking the square wave and sinusoidal wave reference signal, the results are shown in Fig.10a, and Fig.10b.

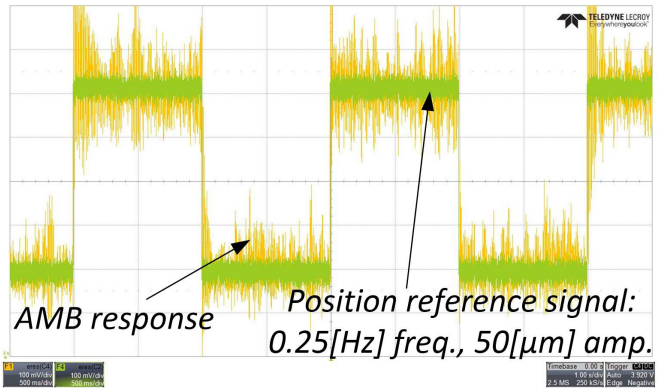

(a) Squre wave tracking

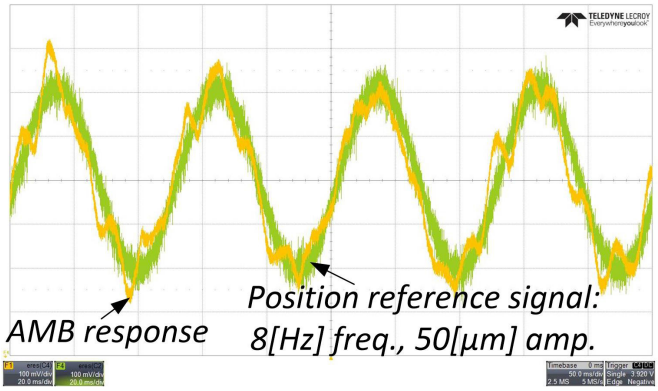

(b) Sinusoidal wave tracking

Fig. 10: Desired AMB position tracking

TABLE I: Parameters of the single-axis AMB

Parameter	Description	Value
m	Moving part equivalent mass	$0.48[kg]$
k	Flexible link stiffness	$1272.8[N/m]$
c	Electromagnetic coefficient	$3.73e-6[Nm^2/A^2]$
g_0	Nominal air gap	$313[\mu m]$
x_f	Add. length due to final permeab.	$1.8634[\mu m]$

V. Conclusion

The AMB power module with an effective current sensor was presented and implemented in this paper. The key idea behind the proposed current sensing method is the sampling of a signal that caries information about the coil current, instead of its full reconstruction. For coil current regulation the optimal controller was designed and implemented. The presented power driver concept was verified experimentally using a real AMB plant.

References

[1] G. Schweitzer and E. H. Maslen, *Magnetic Bearings Theory, Design and Applications to Rotating Machinery*. Springer-Verlag, 2009.

[2] J. Zhang and N. Karrer, "Igbt power amplifiers for active magnetic bearings of high speed milling spindles," in *Industrial Electronics, Control, and Instrumentation, 1995., Proceedings of the 1995 IEEE IECON 21st International Conference on*, vol. 1, 1995, pp. 596–601 vol.1.

[3] J. Y. Hung, N. G. Albritton, and F. Xia, "Nonlinear control of a magnetic bearing system," *Mechatronics*, vol. 13, no. 6, pp. 621 – 637, 2003. [Online]. Available: http://www.sciencedirect.com/science/article/pii/S095741580200034X

[4] J. Zhang and J. O. Schulze, "Synchronous three-level pwm power amplifier for magnetic bearings," in *International Symposium on Magnetic Bearings*, 1996.

[5] Z. Changsheng and M. Zhiwei, "A pwm based switching power amplifier for active magnetic bearings," in *Electrical Machines and Systems, 2005. ICEMS 2005. Proceedings of the Eighth International Conference on*, vol. 2, 2005, pp. 1563–1568.

[6] Z. Changsheng, C. Yang, Z. Dan, and C. Liang, "A current-control mode three-level pwm switching power amplifier for active magnetic bearings," in *Electrical Machines and Systems, 2008. ICEMS 2008. International Conference on*, 2008, pp. 2217–2220.

[7] J. Wang and L. Xu, "Analysis and modeling of a switching power amplifier for magnetic bearing," in *Industrial Electronics and Applications, 2009. ICIEA 2009. 4th IEEE Conference on*, 2009, pp. 2257–2261.

[8] L. Zhang, K. Liu, and X. Chen, "Fpga implementation of a three-level power amplifier for magnetic bearings," in *Electronic Measurement Instruments, 2009. ICEMI '09. 9th International Conference on*, 2009, pp. 1–455–1–460.

[9] J. Wang and L. Xu, "System model of three-level switching power amplifier for magnetic bearing," in *Measuring Technology and Mechatronics Automation, 2009. ICMTMA '09. International Conference on*, vol. 2, 2009, pp. 708–711.

[10] D. Wang, F. Wang, and Y. Zhao, "Study on three-level power amplifier of magnetic bearings for high speed machine," in *Computer Science and Information Technology (ICCSIT), 2010 3rd IEEE International Conference on*, vol. 1, 2010, pp. 607–612.

[11] W. Yu, Y. Fan, S. Liu, and D. Li, "Research on matlab simulation of three level power amplifier for magnetic bearing," in *Power and Energy Engineering Conference (APPEEC), 2010 Asia-Pacific*, 2010, pp. 1–4.

[12] M. Peretz and S. Ben-Yaakov, "Time-domain design of digital compensators for pwm dc-dc converters," *Power Electronics, IEEE Transactions on*, vol. 27, no. 1, pp. 284–293, 2012.

[13] S. Lei and A. Palazzolo, "Real time digital control of magnetic bearings with microprocessors," in *Innovative Computing, Information and Control, 2006. ICICIC '06. First International Conference on*, vol. 2, 2006, pp. 154–157.

[14] W. Zhang, Y. Dun, Y. Sun, L. Yu, W. Shi, W. Zhang, and M. Shi, "High productivity reconfigurable digital control system and its application on magnetic bearing," in *Industrial Electronics and Applications, 2009. ICIEA 2009. 4th IEEE Conference on*, 2009, pp. 1844–1850.

[15] L. Zhang and J. Fang, "Pwm power amplifier with pd correction for magnetic suspending flywheel," vol. 5253, 2003, pp. 741–746. [Online]. Available: http://dx.doi.org/10.1117/12.521984

[16] A. Bonfitto, G. Botto, M. Chiaberge, L. Suarez, and A. Tonoli, "A multi-purpose control and power electronic architecture for active magnetic actuators," in *Power Electronics and Motion Control Conference (EPE/PEMC), 2012 15th International*, 2012, pp. DS2b.9–1–DS2b.9–5.

[17] D. Trumper, S. Olson, and P. Subrahmanyan, "Linearizing control of magnetic suspension systems," *Control Systems Technology, IEEE Transactions on*, vol. 5, no. 4, pp. 427 –438, jul 1997.

[18] R. W. Erickson and D. Maksimovic, *Fundamentals of Power Electronics (Second Edition)*, 2nd ed. Springer, 2001. [Online]. Available: http://www.worldcat.org/isbn/0792372700

[19] B. Mammano, "Current sensing solutions for power supply designers," Texas Instruments Incorparated, Tech. Rep., 2001.

[20] P. Ripka and A. Tipek, *Modern Sensors Handbook*. Wiley-ISTE, 2007.

[21] S. Ziegler, L. Borle, and H. H. C. Lu, "Transformer based dc current sensor for digitally controlled power supplies," in *AUPEC*, 2007.

[22] K. Ogata, *Modern Control Engineering (4th edition)*. Prentice-Hall, Inc. Upper Saddle River, New Jersey, 2002.

[23] A. Locatelli, *Optimal Control An Introduction*. Birkhauser Basel, 2001.

[24] J. P. Hespanha, *Linear systems theory / Joao P. Hespanha*. Princeton